Biomechanics of Brain Injury from the Reconstruction of Three Pedestrian-Car Collisions

Claire E. Baker, Phil Martin, Mark Wilson, David J. Sharp, Mazdak Ghajari

I. INTRODUCTION

Each year 1.2 million people die in Road Traffic Collisions (RTCs) globally (2.1% of global mortality) with a further 50 million casualties [1]. Head and brain injuries in particular cause life-altering injuries and increase the odds of being fatally injured by 6.3 times compared to non-head injuries. Despite making up a small proportion of road users, Vulnerable Road Users (VRUs) account for 20–25% of fatalities [2]. All VRUs, particularly pedestrians, are at greater risk of sustaining head injuries during collisions due to reduced head protection. Computational collision reconstruction enables the kinematics of the body interacting with the vehicle to be understood. Biomechanical metrics can be used to quantify injuries [3]. Both are important to guide informed injury prevention strategies.

II. METHODS

Method Overview

We selected three pedestrian-car collision cases with different TBI severity from the detailed Road Accident In-Depth Study (RAIDS) database. We reconstructed these three collisions with multibody simulation software PC Crash 11.0. We used measurements, speed calculations and CCTV footage where available to reconstruct the collisions. We compared observed and simulated throw distances, times and locations of head impacts. We examined the 3D linear and rotational accelerations and related quantities based on these biomechanical properties for each case. Examples include the Head Injury Criterion (HIC), Brain Injury Criterion (BrIC) and the peak velocities and accelerations (PLV, PRV, PLA and PRA). We compared true injuries casualties sustained to injuries predicted from these metrics.

Data Sources

STATS19 is Great Britain's (GB) database of all nationally reported collisions. We use STATS19 to find common pedestrian collision configurations. RAIDS is a UK Government Department for Transport initiative to collect in-depth RTC data. Information about the scene of the collision, environmental factors, the vehicles and details of the injuries sustained by casualties is collected and entered by trained collision investigators to ensure high accuracy. The extremely detailed information regarding the vehicle velocities, impact points and rest positions makes RAIDS an extremely valuable tool for studying the injuries sustained in RTCs and the injury mechanisms through accident reconstruction.

Pedestrian Collisions in Great Britain

We analysed STATS19 collision data from March 2013 to December 2018. Over this 69-month period there were 142,604 pedestrians involved in reported collisions. The GB annual pedestrian casualty average is therefore approximately 25,000. 21,000 (85%) of these casualties were injured in 30mph zones. 11,000 (45%) pedestrians with known movement were crossing from the driver's nearside (most common movement). Omitting unknown locations, we found 11,000 (48%) pedestrian collisions occurred while crossing a carriageway away from a designated facility. 3,700 (16%) occurred on a crossing facility. 2,800 (11%) occurred off-road while the pedestrian was on a footway or verge. This exploratory analysis enabled us to reconstruct cases that are very relevant to GB's collision landscape.

Case Selection

When accessed on 4 April 2019, RAIDS contained 1,856 accidents involving 3,521 vehicles. Of ~5,000 people involved in these RTCs, there were 2,516 casualties including 113 pedestrians. We selected pedestrian cases that were common in the GB collision landscape to maximise study impact. We ensured selected cases occurred in 30mph speed limit areas at the three most common location types, with the most common crossing direction (where applicable). CCTV was prioritised. We chose cases with different TBI severity: Case 1 (no TBI, AIS0); Case 2 (mild TBI, AIS2); and Case 3 (moderate-severe

C. Baker (c.baker17@imperial.ac.uk, +44(0)1344 770 140) is a PhD student in Engineering and M. Ghajari is a Senior Lecturer in Biomechanics and Design Engineering at Imperial College London. P. Martin is a researcher in Biomechanics at the Transport Research Laboratory Ltd., Crowthorne, UK. M. Wilson is a Consultant Neurosurgeon and D. Sharp is a Professor of Neurology in Medicine at Imperial College London.

TBI, AIS5). All head injuries were attributed with high confidence primarily to vehicle not ground contact by the collision investigator. All casualties were adult males struck by M1 passenger vehicles.

PC Crash Modelling

We used physical evidence, such as vehicle damage patterns and CCTV footage, and collision investigator analysis to reconstruct the collisions. The DSD2016 catalogue was used to select the exact make, model and spec of the vehicle in each case. Accurate front-end geometry is given by the vehicle mesh. We used default values of the vehicle's centre of gravity and kerb weight unless RAIDS specified otherwise. The pedestrian multibody system used consists of 20 ellipsoids connected via ball-and-socket and hinge joints [4]. Joint stiffness of the ankle, knee and hips was adjusted to match motion type [5-7]. The input age, height and weight adjust the model's body data according to the report "International Data on Anthropometry" [8]. PC Crash 11.0's kinetic model was used to calculate the vehicle and multibody system's motion. The model calculates the contact force from the penetration between the multibody system and vehicle surface based on a linear stiffness function. The coefficient of restitution for pedestrian impact was taken from experimental tests using dummies [9]. Other parameters were coefficient of friction (road-tyre): 0.8 (dry, hot-rolled asphalt), coefficient of friction (car-pedestrian): 0.2, coefficient of friction (road-pedestrian): 0.6 and integration timestep: 0.1 ms.

III. INITIAL FINDINGS

Case 1 The collision occurred when a passenger car turned right into a side road at 10mph, hitting the pedestrian who was running across the side road. His head hit the A-pillar before he fell to the ground (Fig. 1). The car sustained damage to the driver side headlight casing, a dent to the A-pillar and the wing mirror was folded back. The pedestrian bruised his left ankle, his right thigh and his forehead. A CT scan found no TBI and no further symptoms were reported. He was 1.65m tall and weighed 70kg.

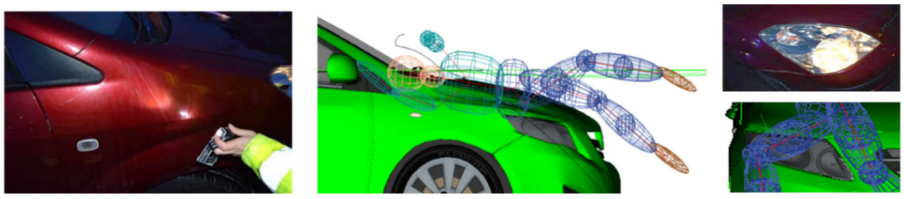

Fig. 1. Case 1 damage and corresponding matched multibody PC Crash simulation.

Physical damage to the left dipped beam bulb was matched in the simulation by the contact with the right thigh (Fig. 1). The wing mirror was folded back. In the simulation, the hand experienced a force of 445.23 N from hitting the wing mirror. Table I compares observation and simulation metrics.

Case 2 The pedestrian ran straight across a pedestrian crossing without signal to cross and collided with a car travelling at 24.53 mph. The pedestrian was thrown upwards, rotated 360° before landing 13.0 ± 1.0 m from the point of collision, ahead of the stopped car. The pedestrian's right leg hit the front of the car, causing his head and shoulder to contact the windscreen 0.167 ± 0.041 s later (Fig. 2). The pedestrian was conscious when paramedics arrived. He sustained an intracranial bleed and right-sided temporal/occipital haematoma. Speed, distances and pedestrian height (1.75m) were measured from the 24 fps CCTV. His weight was estimated as 70kg from his slight-to-average build. Access to CCTV of the full impact enabled strong comparison between the observed and simulated collision. Table I shows superb agreement for Case 2 head impact time, location and pedestrian throw distance.

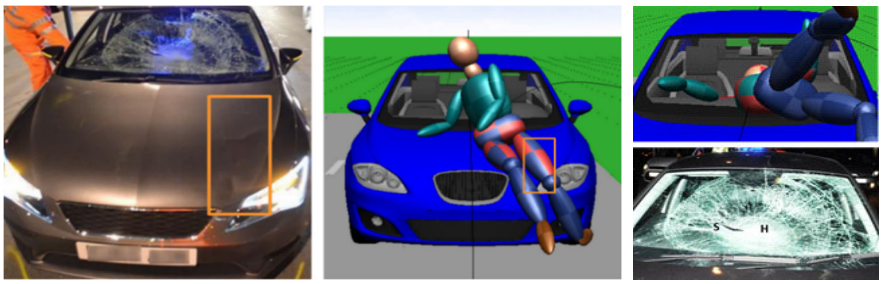

Fig. 2. Case 2 damage profile used to position the pedestrian multibody.

Case 3 Speed was calculated from vehicle movement immediately prior to the RTC captured on CCTV. The car lost control, mounted the pavement and impacted the pedestrian from behind, left knee first. His head contacted the windscreen before he was thrown 14.34 m. The pedestrian was found unresponsive (GCS3), lying on his left side by paramedics. His pupils were equal and reactive. He sustained four serious head injuries: large right-sided epidural haematoma (AIS5), right-sided frontal subdural haematoma (AIS3), complex temporal bone fracture (right temporal mandibular joint and middle ear cavity) (AIS3) as well as frontal and temporal lobe contusions bilaterally (AIS3). His height was noted as 'short-to-medium'. We allocated a height of 1.70m and the average weight (75kg). The same approach detailed in Case 2 was used for reconstruction (not reported for brevity).

TABLE I
GOOD AGREEMENT OF OBSERVED AND SIMULATED HEAD IMPACT TIMES, LOCATIONS AND THROW DISTANCES.

Comparison Metric	Case 1		Case 2		Case 3	
	Observed	Simulated	Observed	Simulated	Observed	Simulated
Head Impact Time (s)	Unknown	0.228 ± 0.036	0.167±0.042	0.142±0.036	Unknown	0.119±0.036
Head Impact Location (coordinates from ref point, m)	A-pillar (0.08, -0.10) from window edge	A-pillar (0.05, 0.06) from window edge	0.68 ± 0.05 from LHS, 28.1–52.5% from base	0.68 ± 0.05 from LHS, 29.7–54.1% from base	0.31 ± 0.08 from LHS, 34.3–61.0% from base	0.38 ± 0.05 from LHS, 21.3–57.4% from base
Pedestrian Throw (m)	<2 (to side)	1.41	13.0 ± 1.0	12.7 ± 1.0	14.3 ± 0.5	14.2 ± 0.3

Comparison Between Pedestrian-Car Collision Cases

We compare seven head injury measures that incorporate acceleration, velocity and forces. The PLA value in each case increases from Case 1 to Case 3. The HIC value increases ~20 times from 36.59 to 742.31 between Cases 1 and 2, before approximately doubling to 1314.39 in Case 3. The PRA in Case 1 (3.8 krad/s^2) was comparable to that in Case 2 (3.7 krad/s^2) despite different TBI severities. In Case 3 the pedestrian sustained an AIS5 injury and the PRA was over 5 times higher than Cases 1 and 2, at 20krad/s^2. Although Cases 1 and 2 had similar PRA values, there was an almost three-fold increase in the PRV between Cases 1 and 2. As with the PRA, Case 3 exhibits a much higher rotational velocity of 64.18 rad/s. The BrIC values also increase for each successive case from Case 1 to Case 3. The contact force increases by 2.3–2.4 times from Cases 1 to 2 and 2 to 3, supporting skull fracture only in Case 3.

TABLE II
CALCULATED BIOMECHANICAL HEAD INJURY METRICS. INCREASE SEEN FROM CASE 1 TO CASE 3.

Injury Metric	Case 1	Case 2	Case 3
Peak Linear Acceleration (PLA)	49.62 g	119.75 g	201.40 g
Head Injury Criterion (HIC)	36.59	742.31	1470.89
Peak Rotational Acceleration (PRA)	3.829 krad/s^2	3.698 krad/s^2	20.461 krad/s^2
Peak Rotational Velocity (PRV)	10.24 rad/s	28.82 rad/s	64.14 rad/s
Brain Injury Criterion (BrIC), BrIC (2015 Revision)	0.259, 0.317	0.523, 0.714	1.08, 1.90
Peak Resultant Force (PRF)	2.604 kN	6.542 kN	15.455 kN

IV. DISCUSSION

We present three case studies which are representative of common GB pedestrian collisions. We demonstrate that with comparison to CCTV footage available, our reconstructions reproduce key times and locations from the collisions accurately, with almost all simulated metrics within the uncertainty of the observed result. We predict the pedestrian in Case 1 not to sustain a TBI (below even 25% concussion threshold) [10-11]. The pedestrian in Case 2 is predicted to have just less than 50% risk of sustaining an AIS2+ injury from the PLA (threshold for 50% risk of AIS2+ is 116g [12]) and HIC measurement of 742 (threshold for 50% risk of AIS2+ is 825 [13]). The HIC of 742 is also above Marjoux's 2008 threshold for 50% risk of brain injury of 533 [14]. Rotational metrics (PRV in Case 2 of 28.82 rad/s) again predict the Case 2 pedestrian to be slightly below the AIS2/3 threshold [15]. The BrIC value of 0.714 gives a corresponding risk of AIS3+ of 32% [16]. The PRF of 6.542kN is just above

the average skull fracture threshold across the involved parietal, occipital and frontal bones (ranging from 4.5 kN to 14.1 kN with males tending to have higher peak loading required for fracture) [17]. From all metrics, we predict the Case 2 pedestrian to have a 50% risk of sustaining an AIS2 injury, with no bridging vein rupture or subdural haematoma [18-20], as observed. While there is a skull fracture risk, as a young adult male this fracture is likely to have required above average contact force.

Case 3 had the highest PLA (201.40g) which predicts a 5–40% risk of sustaining skull fracture (180 g– 250 g) [18]. The risk of skull fracture is supported by the peak PRF of 15.5kN lying above the 12kN thresholds for occipital fracture [21-22]. SDH is also predicted from the PLA >130g [23]. This is supported by the PRV of 64.18 rad/s, which in combination with PRA is above thresholds for bridging vein rupture [19-20]. However, the HIC value in Case 3 (1314) was approximately 10% below the 50% skull fracture and SDH risk thresholds (1450 and 1429, respectively). As rotational acceleration is known to influence bleeding within the brain, it is possible that HIC's purely linear component may not fully characterise the injury risk. HIC of 1314 also underestimates the severity of the injury sustained, predicting AIS2–3 and a 50% risk of serious neurological injury [14]. Using the method specified above, BrIC of 1.89 gives a 99.9% risk of sustaining AIS4+ and a 97.9% risk of sustaining AIS4+ injury, respectively. Most biomechanical metrics in our analysis therefore predict the patient to sustain SDH, skull fracture with an overall severity of AIS3+, as was the case clinically. HIC as a metric predicted a slightly below 50% risk of skull fracture, SDH and suggested AIS2–3 as opposed to the AIS5 sustained, which should be further examined. There is some discrepancy between biomechanical metrics and prediction outcomes, particularly when predicting bleeding and overall head injury severity using linear metrics. This is not surprising as rotation is known to influence brain injury severity, particularly bleeding. In general, the biomechanical metrics well match injuries in all cases.

Limitations and Ongoing Work

Our future work will include detailed reconstructions using MADYMO, because PC Crash is limited in its ability to model unloading during surface interactions between specific body parts and vehicle. This approach will allow us to extract the 3D linear and rotational accelerations of the head during the collision. These accelerations can be used to load high-fidelity Finite Element (FE) models of the head and brain [24]. We will use FE models to analyse the brain's response to the forces experienced during the collision. Despite all casualty head injuries attributed primarily to the vehicle strike and the magnitude of the ground strike being less than 30% of that of the vehicle strike, it is likely that the ground still contributes to injury. We can use this FE approach to assess the level of strain within the brain during the ground and vehicle impact. MADYMO will also give us the capability to perform parametric sweeps when values for height and/or weight of the pedestrian are not known precisely. Combining collision reconstruction with computational brain injury modelling for case studies that are representative of collisions in GB as a whole will allow us to better understand the biomechanics of traumatic brain injury of VRUs in the real world and design more effective protection strategies.

V. ACKNOWLEDGEMENTS

The authors acknowledge the EPSRC funding received from the CDT Neurotechnology, the Transport Research Laboratory funding, and the access to the RAIDS database from the Department for Transport.

VI. REFERENCES

[1] Peden, M., *et al*., *Inj Prev*, 2004.
[2] SEC, European Road Safety Action Programme, 2006.
[3] Gabler, J., *et al*., *Ann Biomed Eng*, 2018.
[4] Steffan, H., PC Crash Operating and Technical Manual, 2016.
[5] Bergmann, G., *et al*., *J Biomech*, 1993.
[6] Günther, M., *et al*., *J Appl Biomech*, 2002.
[7] Stefanyshyn, D., *et al*., *J Appl Biomech*, 1998.
[8] Juergens, H., *et al*., International Labour Organisation, 1990.
[9] Lucchini, E., *et al*., US Department of Transportation, 1976.
[10] King, A., *et al*., IRCOBI, 2003.
[11] McAllister, T., *et al*., *Ann Biomed Eng*, 2012.
[12] Peng, Y., *et al*., IRCOBI, 2012.
[13] Chinn, B., *et al*., European Commission, 2001.
[14] Marjoux, D., *et al*., *Accid Anal Prev*, 2008.
[15] Ommaya, A., *et al*., *Int J Impact Eng*, 1994.
[16] Mueller, B., *et al*., ESV Conference, 2015.
[17] Yoganandan, N., *et al*., *SAE Transactions*, 1988.
[19] Löwenhielm, P., *J Bioeng*, 1978.
[20] Ommaya, A., *et al*., *J Appl Biomech*, 1971.
[21] Yoganandan, N., *et al*., *SAE Transactions*, 1994.
[22] Advani, S., *et al*., Human Body Dynamics, 1982.
[23] Willinger, R., *et al*., *Int J Crashworthiness*, 2003.
[24] Ghajari, M., *et al*., *Brain*, 2017.